

# Refiner Plate Clash Detection Using an Embedded Force Sensor

**Dustin Olender, Paul Francescutti and Peter Wild**

University of Victoria, BC, Canada

**Peter Byrnes**

Herzberg Institute of Astrophysics, Victoria, BC, Canada

## ABSTRACT

Plate clash in disc refiners continues to detract from the efficiency of mills, reducing plate life and affecting production. The work presented here examines the potential of a piezoelectric-based force sensor for clash prediction. Four sensors were installed in an operational reject refiner over a three-month period at the Catalyst Paper mill in Port Alberni, B.C., Canada. Signals from these sensors were processed for prediction of plate clash and the results were compared to the accelerometer-based plate protection system currently in use at the mill. The force sensors consistently gave advanced warning of a clash event, many seconds before the accelerometer. A sensitivity study showed that the new system was able to outperform the accelerometer system over a range of detection settings, and that the accelerometer could not be tuned to match the performance of the new system.

## INTRODUCTION

Plate clash occurs when the gap between refiner plates is reduced to zero. The resulting metal-to-metal contact causes large forces between the bars on these plates, accelerating wear and disrupting operation (1, 2). This destructive event is thought to be caused by the breakdown of the pulp pad between the refiner plates, and is sometimes called “pad collapse.” The exact mechanisms that induce pad collapse are unknown, but disruptions in pulp flow caused by back-flowing steam are often blamed [1]. Variations of forces in the refining zone could be associated with such a breakdown of the pulp pad. These variations could be used to detect an imminent plate clash and then trigger a reduction of the load on the refiner plates to prevent the clash. Current plate protection systems rely on gap sensors or vibration monitors to detect the onset of clashes. While these devices have proven useful, they do not consistently prevent plate clash [2]. The importance of a reliable and effective plate protection system lies in its ability to extend refiner plate life and produce uniform pulp quality [3]. Accordingly, the goal of this work is to evaluate the potential of a force sensor to predict clash events.

Past efforts to detect clashes include the system currently used in the Port Alberni reject refiners. This method was first developed and tested in 1977 [4]. The system is based on the measurement of vibrations in the refiner body. It was found that a range of vibrational frequencies showed an increase in amplitude prior to, and during, a plate clash [3]. An accelerometer-based system is used to monitor this frequency range and warn of an impending clash if an increase in the amplitude of vibration is detected. Another system that uses information gathered from an accelerometer was developed by Whyte [5]. Whyte’s method detects a drop in vibrational amplitude associated with a reduction in the flow of pulp between refiner plates prior to clash. A third clash detection system was developed by Brenholdt [6]. This system measures electrostatic discharges through the refiner caused by impacts of charged particles in the pulp. Electric impulses are measured directly from the refiner body and have been successfully correlated to pulp properties and gap width.

In the work presented here, four piezo-electric force sensors, known as Refiner Force Sensors (RFS), were installed in a reject refiner at a Catalyst Pulp and Paper mill in Port Alberni, B.C., Canada. Trials were carried out at regular intervals over the three month installation, each trial consisting of a set of controlled experiments. The sensors used in these trials were the fourth generation of sensor described in previous work [7]. The sensors each contain two piezoelectric elements and a thermocouple, and replace a short (5 mm) segment of bar in the refiner plate segment. The sensors are capable of measuring the normal and shear forces experienced by pulp during bar-crossing impacts. High sampling rates are necessary to resolve these impacts, whose durations are on the order of microseconds. However, the resulting force signals also contain information regarding larger timescale phenomena, such as the flow of pulp in the refining zone [8]. Signals from the RFS could therefore contain information regarding process fluctuations associated with plate clash.

## CURRENT PLATE PROTECTION SYSTEM

The plate protection system in use on the Port Alberni refiners is based on the signal from an accelerometer mounted on the outboard bearing block of the refiner. The accelerometer signal is conditioned to produce a plot of the amplitude of vibration in a frequency range known to be associated with clashes [3]. An impending clash is detected using two alarm types. The first alarm type, *alert*, is triggered when the acceleration exceeds a specified *static threshold*. The second alarm type, *danger*, is triggered when the acceleration exceeds a *dynamic threshold*. This dynamic threshold is based on the *running average* which is defined as the average of the accelerations recorded during a prescribed and immediately preceding time period. The dynamic threshold is the sum of the running average and a prescribed fixed offset. The accelerometer-based plate-protection system is illustrated in Figure 1.

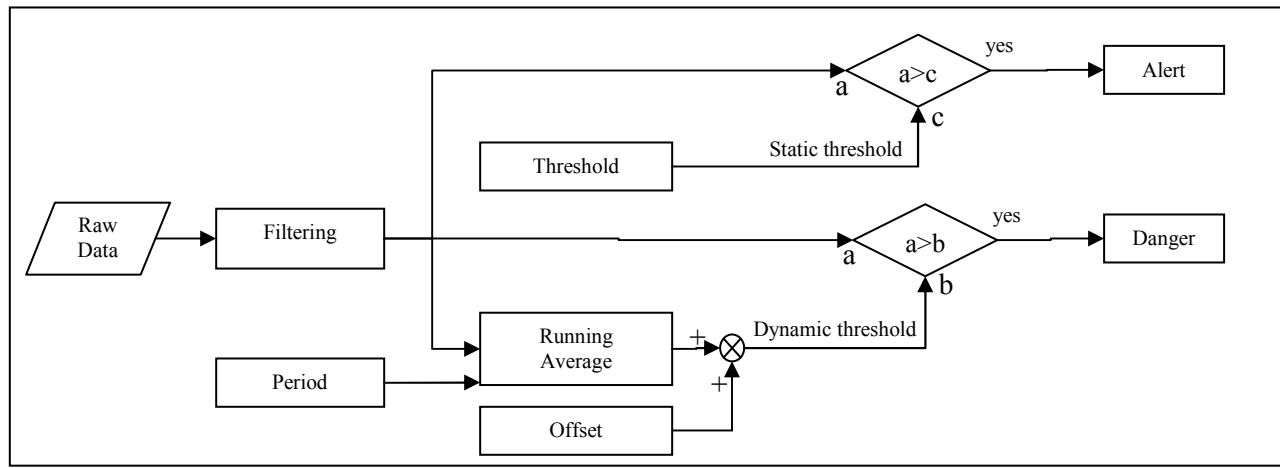
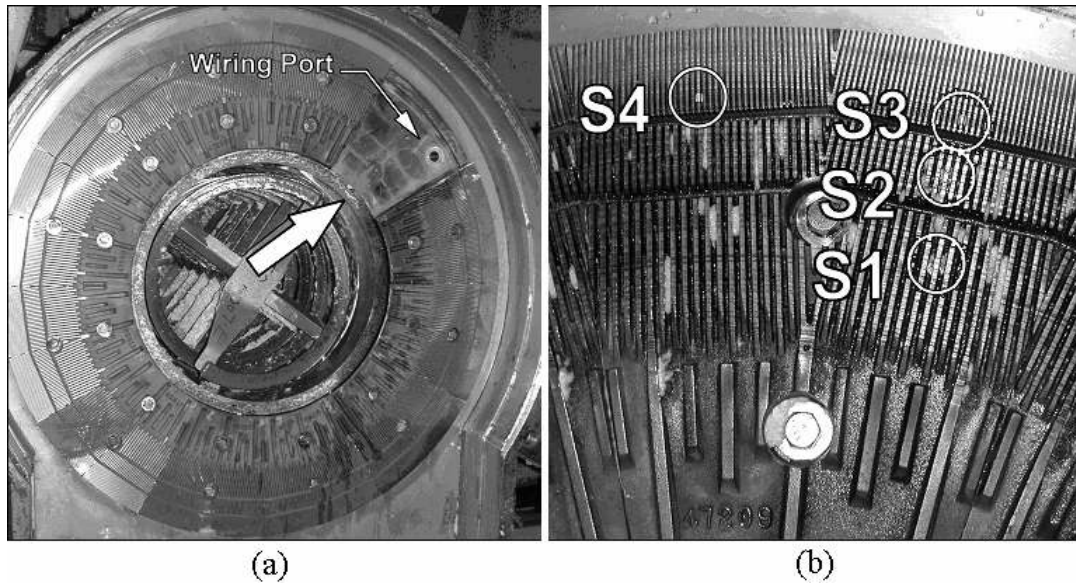


Figure 1. Accelerometer *Danger* and *Alert* alarm detection methods.

During the trials, the static threshold for the Alert was 40 g while the offset for the danger was set at 5 g over the 50 s running average. According to operators at the Port Alberni mill, the alarm of importance is the danger alarm. The alert alarm is seldom triggered during normal operation.

## SENSOR INSTALLATION, DATA ACQUISITION AND PRE-PROCESSING

Four sensors were installed in one plate segment on the stator disc of an Andritz 45-1B refiner. This is a single-disc, atmospheric refiner running at 1800 RPM on which plate gap is controlled mechanically by a lead screw. The instrumented Durametal™ 47209 plate segment remained installed for the entire life of the plates, which was approximately three months (~1800 hours), starting in September and ending in November 2005. The installation took place during a regularly scheduled plate change, and as a result, required little additional downtime. Figure 2a shows the location of the instrumented plate segment and the port used to route wiring outside of the refiner housing. Figure 2b shows the location and identification of each sensor on the plate.



**Figure 2. Location of instrumented plate segment, wiring port and force sensors. (a) Vacant segment position, just prior to installation of the instrumented plate. (b) Location and identification of the sensors in the instrumented plate.**

In the fine bar region of the refiner plates, the bar-crossing frequency was as high as 32 kHz. Because of this, a high sampling rate of 300 KSamples/s was used. Data acquisition hardware used to record the signals from all sensors consisted of a National Instruments high-speed PXI-6251 board and a low-speed PXI-6133 board installed in a PXI system. Software was developed using National Instruments Labview™ to record data from all four sensors, their thermocouples, and the refiner’s plate protection accelerometer.

It was apparent from manual inspection of the recorded RFS signals that the high sampling rate used to resolve individual bar-crossing impacts was not necessary to record the low frequencies associated with the increase in forces preceding a plate clash. The first step in processing the RFS signal was, therefore, to decimate the data files to a more manageable size. All data processing was performed using National Instruments Labview™ software. As mentioned previously, the data from each sensor was recorded at a sampling rate of 300 KSamples/s. The decimated data was equivalent to data sampled at a rate of 300 Samples/s, allowing for a larger time span to be viewed using a desktop computer. In addition to the decimation, the data was rectified to cast all data points into the positive domain.

### **CLASH EVENTS**

As mentioned above, the sensors were operational for the entire plate life of ~1800 hours. However, because of the high sampling rate and finite data storage space, long-term continuous data collection over this period could not be achieved. Instead, data from the four sensors was collected continuously during five short-term periods consisting of daylong controlled experiments. In between these periods, data collection software automatically recorded 10 seconds of data on 15-minute intervals. This data was supplemented with data from the refiner’s plate protection accelerometer as well as notes taken during continuous trials. Data was stored in several files, the largest of which contained approximately seven minutes of continuous data. Of all the data files collected, only four contained clash events, all of which were found early in the trial period. These events were manually classified as either “clashes”, or “interrupted clashes”. The later describes events where the accelerometer successfully detected and prevented a

clash from occurring. In total, nine events were observed including 6 clashes and 3 interrupted clashes. These events were verified using the trial notes.

Figure 3i shows 412 s, or approximately 6.9 minutes, of continuous decimated and rectified data produced by all RFS. Figure 3ii shows the signal recorded from the accelerometer system for the same period of time. Three events of interest are contained in this data. The first two are interrupted clashes, which are easily observed in the accelerometer data as two peaks at points *a* and *b* in the figure. The third event occurs at point *c*, marking the onset of a suspected clash. It is believed that physical contact between plates occurred at or soon after point *c*, based on the response of the RFS signals shown in Figure 3i. It is not understood why the third event was not averted as the previous two were. All three events can be observed in both the RFS and accelerometer data.

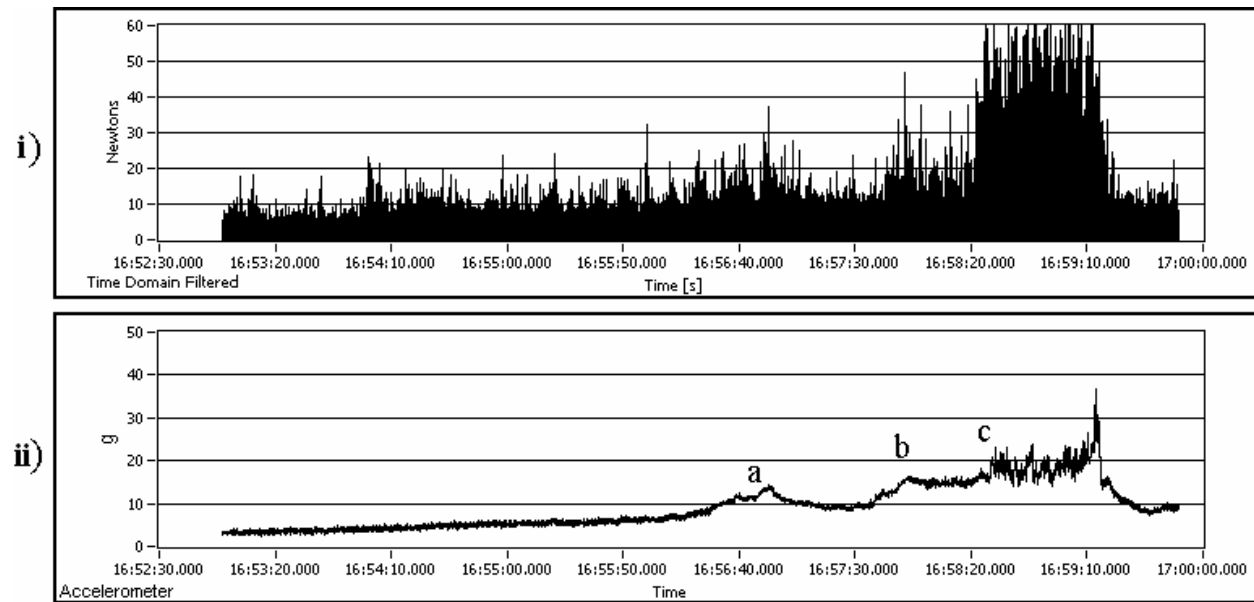


**Figure 3. Samples of i) the decimated and rectified RFS data, and ii) the accelerometer data.**

It is important to note that all clash events analyzed in this work occurred in the first trial period, during run-in of the new refiner plates. Clash events were recorded later in the three-month installation, but none during the continuous acquisition used in the trial periods. These records were therefore incomplete, showing only portions of the clash events, and could not be included in this analysis. It is unknown whether the process conditions in the refining zone that facilitated early detection of plate clash would be affected by plate wear, and this deserves further attention. However, the ability of the RFS to detect these process fluctuations later in the life of the plates was not diminished. All four sensors showed a minimal loss of sensitivity during calibration following the trials.

## **DETECTION METHODS**

Several clash detection algorithms were explored using the RFS data and each was judged based on its ability to predict the clashes before the accelerometer-based plate-protection system. Labview™ software was developed to scan data files and identify clash events. This software also simulated the operation of the accelerometer-based plate-protection system. The accelerometer data was processed and alarms were generated using the threshold and offset definitions described earlier. Figure 4 shows an example of the accelerometer signal and the alarms generated using the simulated clash detection system.

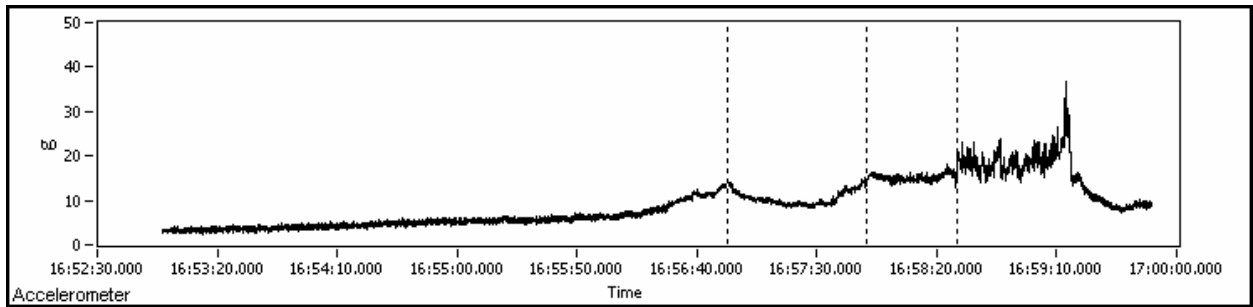


**Figure 4. Accelerometer signal with danger alarms indicated as dashed lines.**

In this figure, each of the three vertical lines indicates a danger alarm as described earlier. The first two peaks are believed to be instances where the accelerometer detected and prevented clashes as previously discussed. The third alarm corresponds to the beginning of an event in which the plate protections system failed to avert a clash. These results give confidence that the simulated accelerometer-based warning system is an accurate simulation of plate protection.

The RFS-based clash detection methods explored in this work are: *peak density*, *weighted peak density*, *running average* and *combined running average*. In all of these methods, the data is first decimated, as mentioned earlier, and then rectified. In the following descriptions of the individual methods, this decimated and rectified data is referred to as the *pre-processed data*.

### **PEAK DENSITY METHOD**

The *peak density* method is based on an *adaptive threshold*. This adaptive threshold is defined as a multiple of the running average of the pre-processed data. A LabView<sup>TM</sup>-based peak detection algorithm<sup>1</sup> is used to identify peaks in the pre-processed data. Each peak that exceeds the adaptive threshold is counted and the number of peaks counted in a prescribed period of time is defined as the *peak density*. This method is illustrated in Figure 5.

<sup>1</sup> The core of the peak-finding algorithm consists of fitting a parabola to successive groups of points. The function checks whether each parabola is at a local maximum, determines the sign of the quadratic coefficient, which indicates the parabola's concavity, and finally checks that the peak is above the designated threshold.

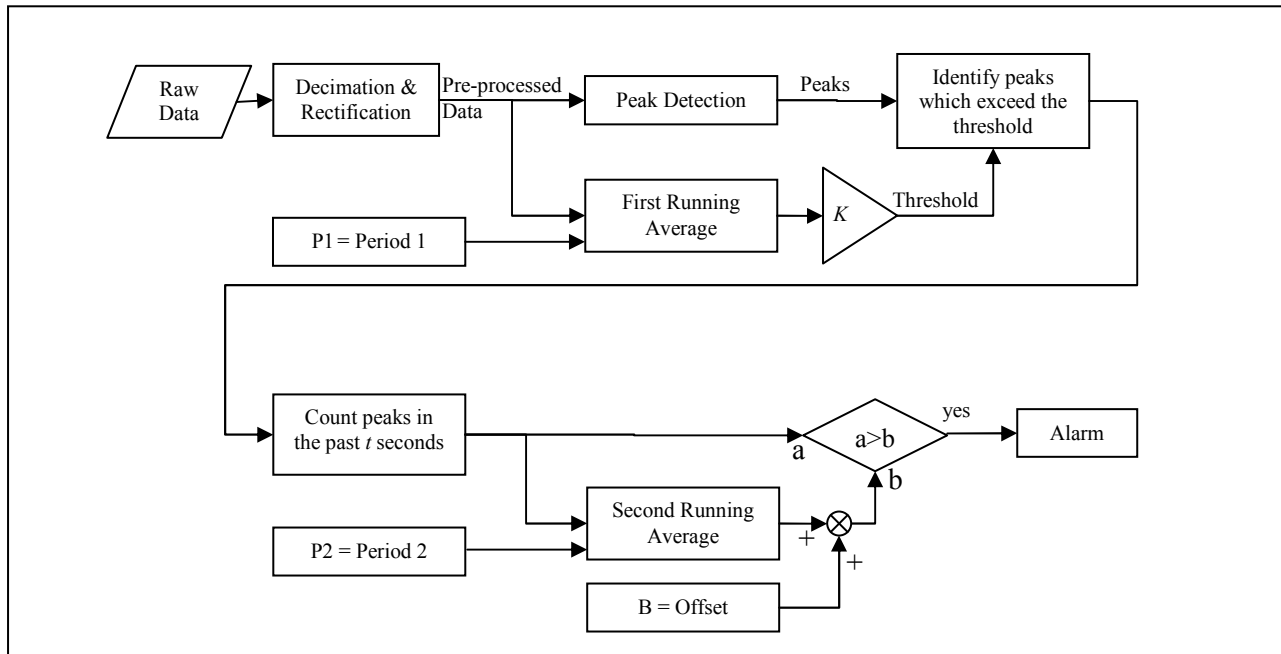


**Figure 5. Data processing strategy used for the Peak Density Method.**

An example of the parameters used to generate the peak density signal is as follows: *The number of peaks in the past  $t = 1.65$  s which exceed the first running average, taken over a period  $P1 = 60$  s, by a factor  $K$  of 4. Alarms are triggered using a second running average, taken over a period  $P2 = 30$  s, and offset value  $B$  of 9 peaks.*

### **WEIGHTED PEAK DENSITY METHOD**

The *weighted peak density* method is an extension of the peak density method. In the peak density method, all peaks above the dynamic threshold, regardless of amplitude, contribute equally. In the weighted peak density method, the contribution of each peak above the dynamic threshold is weighted according to its height. More specifically, weighted peak density is defined as the peak density multiplied by the average peak height during the period over which density is calculated. This method is illustrated in Figure 6.

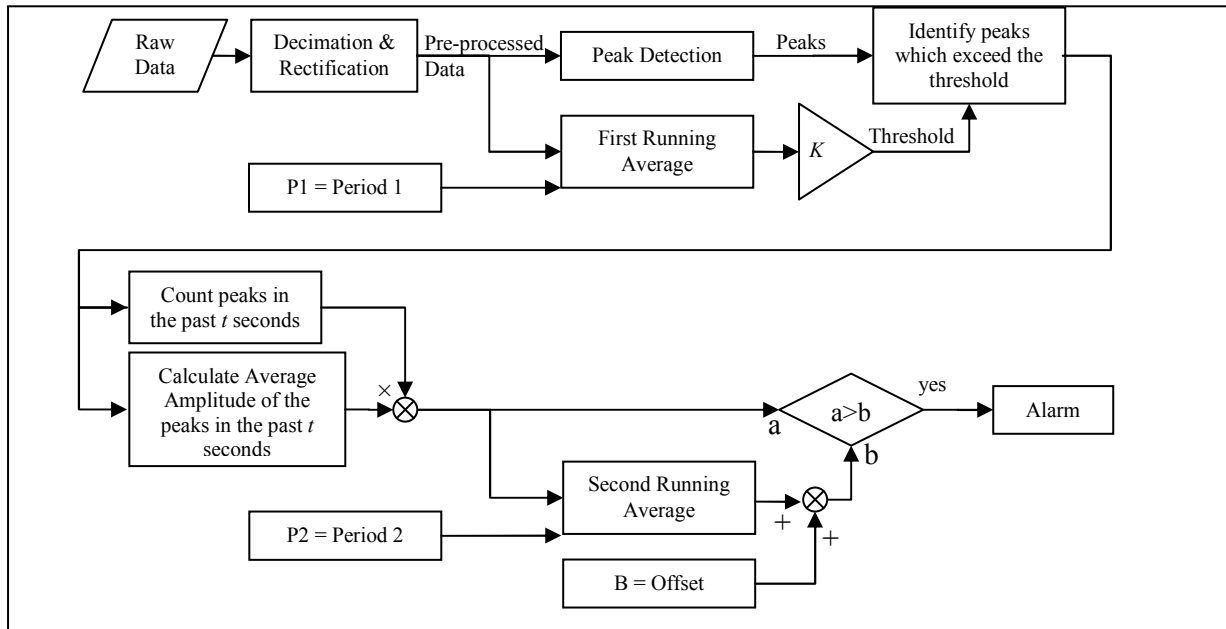


**Figure 6. Data processing strategy used for the Weighted Peak Density Method.**

An example of the parameters used in the weighted peak density method is as follows: The number of peaks in the past  $t = 1.65$  s which exceed the first running average, taken over a period  $P1 = 60$  s, by a factor  $K$  of 4 multiplied by the average height of those same peaks. Alarms are triggered using a second running average, taken over a period  $P2 = 10$  s, and offset value  $B = 80$  N peaks.

### RUNNING AVERAGE METHOD

This method is essentially the same as the method used for the accelerometer-based detection system. In this method, a *first running average* of the pre-processed data is calculated. A *second running average* is then performed on the first running average data. The period over which each of these averages is calculated is longer for the second running average than for the first. Thus, the second running average data is subjected to more “smoothing” than the first running average data. A dynamic threshold is then calculated as the sum of the second running average data and a prescribed fixed offset. When the first running average exceeds this dynamic threshold, an alarm is generated. This process is performed on each sensor signal, two signals per sensor, such that eight independent alarm signals are produced. This method is illustrated in Figure 7.

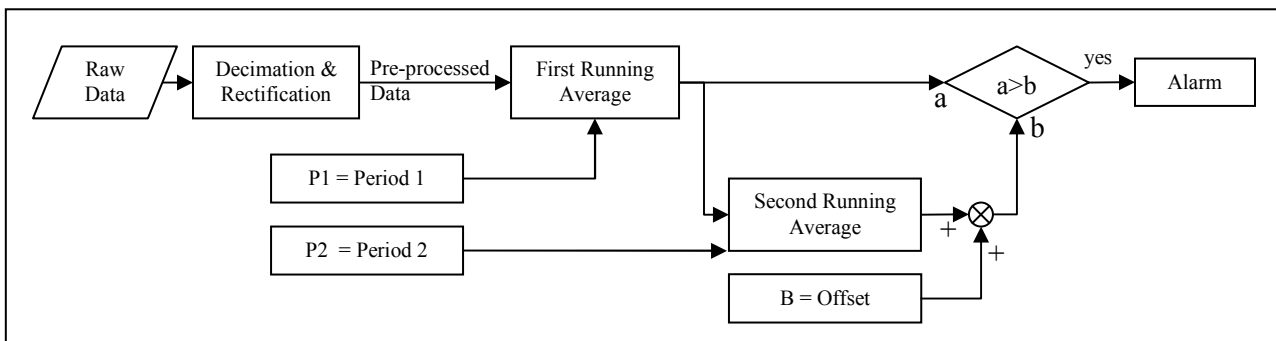


**Figure 7. Data processing strategy used for the Running Average Methods.**

## COMBINED RUNNING AVERAGE METHOD

The *combined running average method* is based on the running average method. Shear and normal force data for the eight signals from the four sensors are pre-processed. The averages of the pre-processed signals are then calculated for each sensor (i.e. the average of the pre-processed shear and normal force signals) and for all four sensors (i.e. the average of the pre-processed shear and normal force signals for all four sensors). These average pre-processed signals are then used to detect impending plate clashes using the running average method, as described above.

## RESULTS

The plots shown in Figure 8 show 412 s, of data from the accelerometer (Figure 8i) and force sensors (Figures 8ii-8vi), as processed with the methods described in the previous section. Note that, in this figure, dashed lines indicate the point at which the simulation of the accelerometer-based method detects an imminent clash and the solid lines indicate the point at which RFS-based methods detect an imminent clash. The time between a solid line and a corresponding dashed line indicates the time by which each RFS-based method leads the accelerometer-based method for each event. From this point forward, this time will be referred to as the *lead time*.



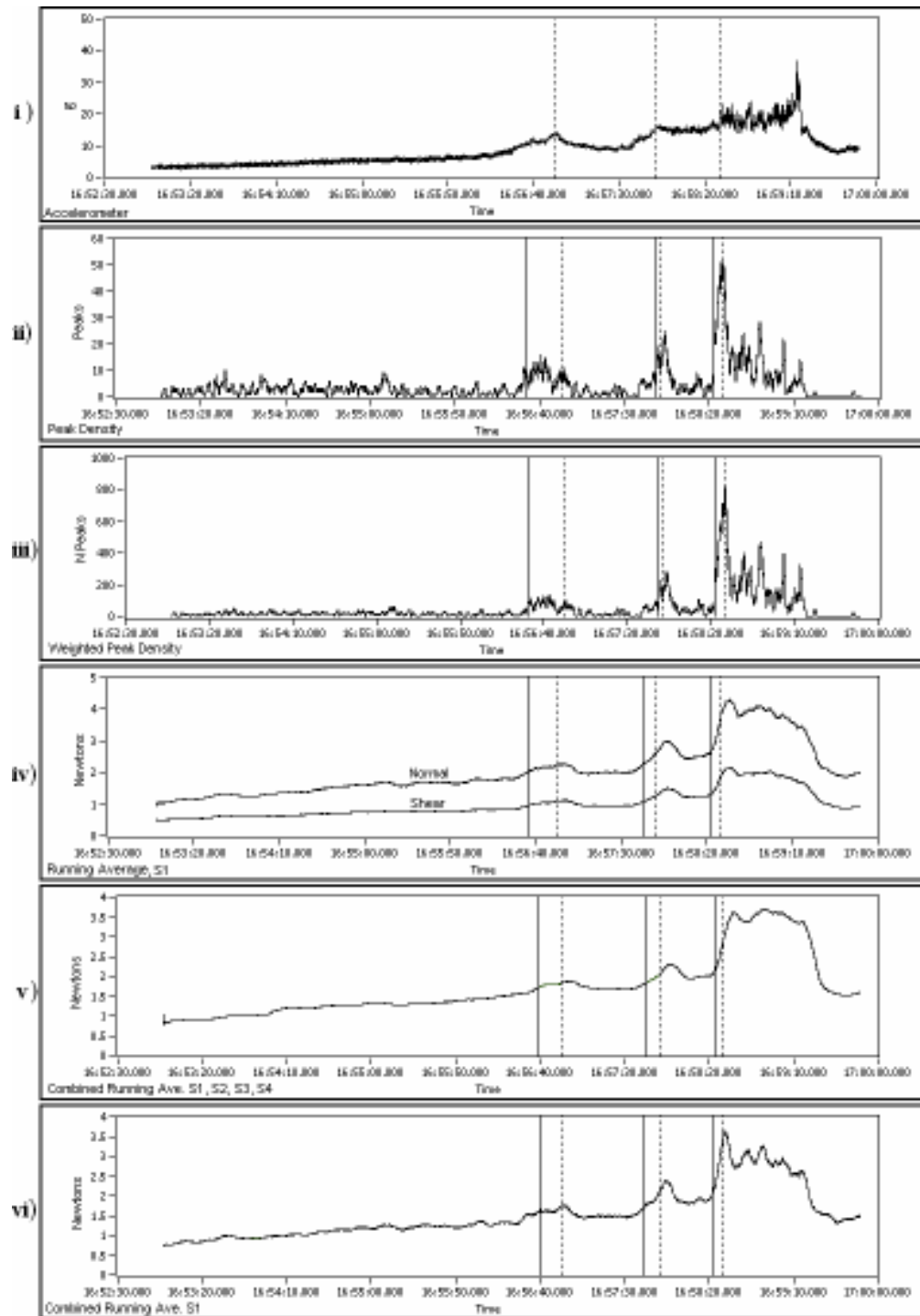


Figure 8. Examples of the output from i) the accelerometer, ii) Peak Density, iii) Weighted Peak Density, iv) Running Average v) Combined Running Average S1, S2, S3, S4 and vi) Combined Running Average of S1. In all figures accelerometer-based Danger alarms are shown by dashed lines, while RFS-based alarms are shown by solid lines.

The performance of each of the five RFS-based detection methods for each of the nine clash events is summarised in Table 1. The lead times presented in Table 1 are based on parameters which were chosen to provide maximum sensitivity without the appearance of false triggers. The accelerometer danger alarm, which is the reference-case for calculation of lead time, was triggered by accelerations greater than 5 g over the 50 s running average. This is the setting used in the mill during the sensor trials.

**Table 1. Lead times<sup>2</sup> for nine clash events using the five clash detection methods.**

Event Designation	Detection Methods				
	Peak Density (S1-normal force) <sup>3</sup>	Weighted Peak Density (S1-normal force) <sup>4</sup>	Running Average (S1 - normal force) <sup>5</sup>	Combined Running Average (S1, S2, S3 & S4 - normal & shear force) <sup>6</sup>	Combined Running Average (S1 - normal & shear force) <sup>7</sup>
a	21.1	22.3	16.8	13.7	12.9
b	2.1	1.4	7.8	7.6	9.3
c	5.9	6.1	5.5	5.2	6.1
d	9.7	9.7	-4.5	5.9	7.5
e	20.0	20.0	23.1	23.1	24.7
f	13.43	-0.84	-1.7	-2.6	11.2
g	-0.57	-0.27	3.2	2.5	15.9
h	-0.020	0.013	1.6	2.3	1.86
i	8.7	9.62	7.4	7.7	8.71
<b>Average Lead Time</b>	<b>8.9</b>	<b>6.3</b>	<b>6.6</b>	<b>7.9</b>	<b>10.9</b>

To further elucidate the performance of the RFS clash detection system, two sensitivity studies were performed. These studies examined the effects of adjusting the key data-processing parameters away from their optimum or reference values. As mentioned above, these optimum values were used to calculate the data in Table 1.

<sup>2</sup> The accelerometer danger alarm, which is the base-case for calculation of lead time, was triggered by accelerations greater than 5 g over the 50 s running average.

<sup>3</sup> Data is generated based on the number of peaks in the past 1.65 s which exceed the current 60 s running average by a factor of 4. Alarms triggered using second running average period of 30 s and offset value of 9 peaks.

<sup>4</sup> Data is generated based on the number of peaks in the past 1.65 s which exceed the current 60 s running average by a factor of 4 multiplied by the average height of those same peaks. Alarms triggered using second running average period of 10 s and offset value of 80 N-peaks.

<sup>5</sup> Data is generated using a first running average period of 10 s on normal force signal from S1. Alarms triggered using second running average period of 15 s and offset value of 0.20 N.

<sup>6</sup> Data is generated using average of signals generated using a first running average period of 10 s on all 8 force signals. Alarms triggered using second running average period of 15 s and offset value of 0.12 N.

<sup>7</sup> Data is generated using average of signals generated using a first running average period of 5 s on normal and shear force signals from S1. Alarms triggered using second running average period of 20 s and offset value of 0.20 N.

In the first study, the accelerometer danger offset was incrementally reduced from its reference value of 5.0 g to a minimum value of 3.25 g. Lead time was calculated relative to the combined running average method based on S1 using the optimum settings listed for Table 1.

In the second study, the RFS alarm offset of the combined running average method based on S1 was incrementally adjusted around its optimum or reference setting of 0.20 N, over the range from 0.15 N to 0.30 N. Lead time was calculated relative to the accelerometer-based method using the settings that were used at the mill during the trials.

In each study and for each incremental adjustment of the key data-processing parameters, the lead time for each of the 9 events was recorded. The average lead time and *number of events led* were then determined. *Number of events led* is defined as the number of events (out of 9) for which the lead time is positive.

The results of the first study are shown in Figure 9. In this figure, the dashed line denotes the offset below which false triggers occur. The results of the second study are shown in Figure 10. As in Figure 9, the dashed line in Figure 10 indicates an offset setting below which false triggers occur.

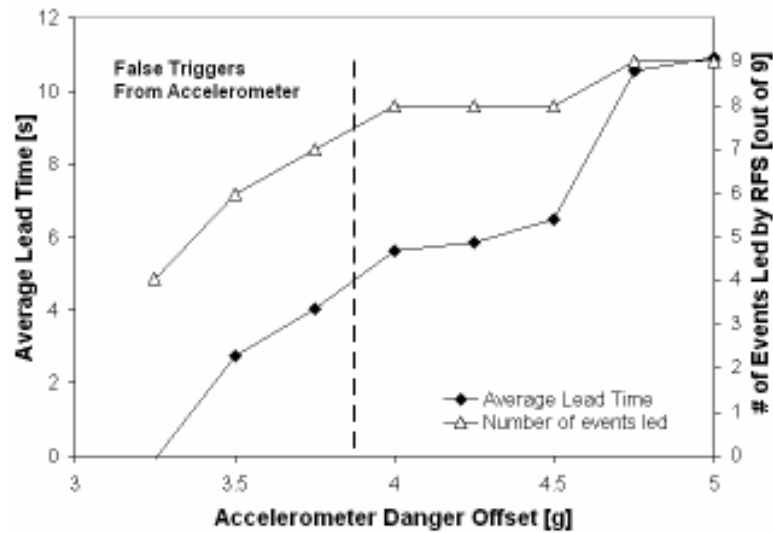


Figure 9. Average lead time and number of events led vs. Accelerometer danger offset.

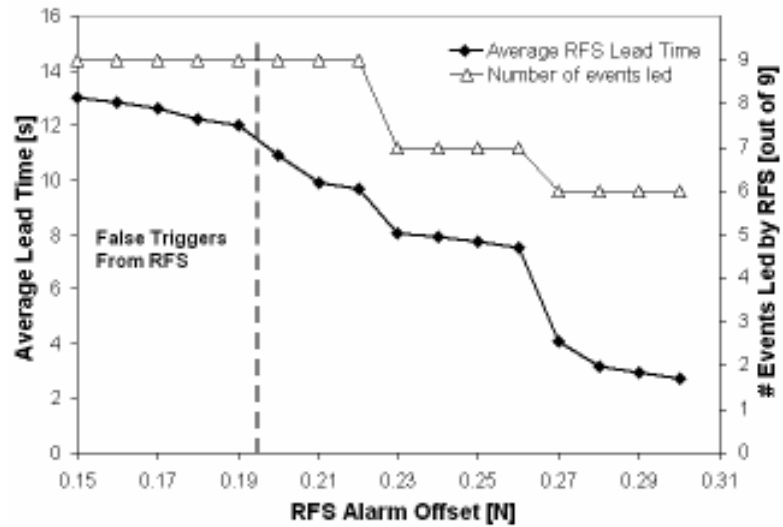


Figure 10. Average lead time and number of events led vs. RFS alarm offset.

## DISCUSSION

The performance of the RFS-based detection methods is superior to the performance of the accelerometer-based system. The average lead times for all of the RFS-based methods are at least 6 seconds. All of the RFS-based detection methods provide positive lead time in at least 7 of 9 events while the combined running average method can detect all 9 events before the accelerometer based method using a single sensor. Each sensor was tested individually as well as in various combinations with other sensors using the combined running average method. It was found that a sensor in the location of S1 provides the greatest increase in clash detection performance based on the number of events led and the average lead time.

The significance of the larger lead times provided by sensor S1 is not completely understood. One hypothesis considers radial location. S1 is the innermost sensor, and the only sensor believed to be completely inside the stagnation point, or the point at which steam velocity is zero. If back-flowing steam is a contributor to the disruption of the pulp pad, it would suggest a restriction of pulp flow radially inward from the stagnation point. This restriction could result in an accumulation of material in the inner part of the refining zone prior to a clash, which would explain the early rise in forces recorded by S1.

The lead time data in Table 1 for events *a*, *b*, *c*, *e*, *g*, *h* and *i* are relatively consistent across all of the detection methods. The data for events *d* and *f*, however, is less consistent. Inconsistencies include the relatively large distribution of lead times found for event *f* as well as the large negative lead time found using the Running Average method on event *d*. These inconsistencies are caused by the presence of local maxima in the processed data as shown in Figure 11. A local maximum may be missed by a small margin leading the detection algorithm to select a second rise in forces following it. Other methods may detect the first maximum leading to a significantly different detection time. This behavior is the result of the characteristics of each detection method and the characteristics of the data surrounding each clash event.

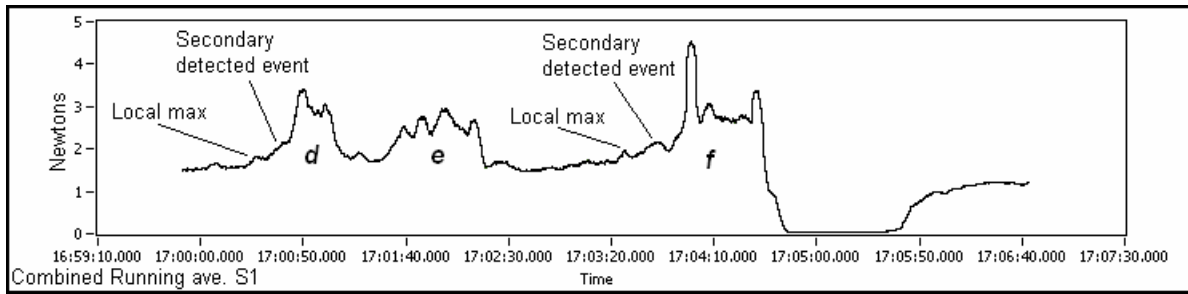


**Figure 11. Detail of local maximums and their potential effect on peak detection performance. Events d, e, and f indicated.**

Another notable characteristic found in the tabulated results is the relatively small lead times for event *h* across all detection methods. This event is characterized by an abrupt increase in force and acceleration amplitudes, as shown in Figure 12. The RFS and accelerometer based system detect the event almost simultaneously, just before the spike in their respective signals. Also noticeable is the similarity in shape between the accelerometer and RFS signals which could also lead to similar detection performance.

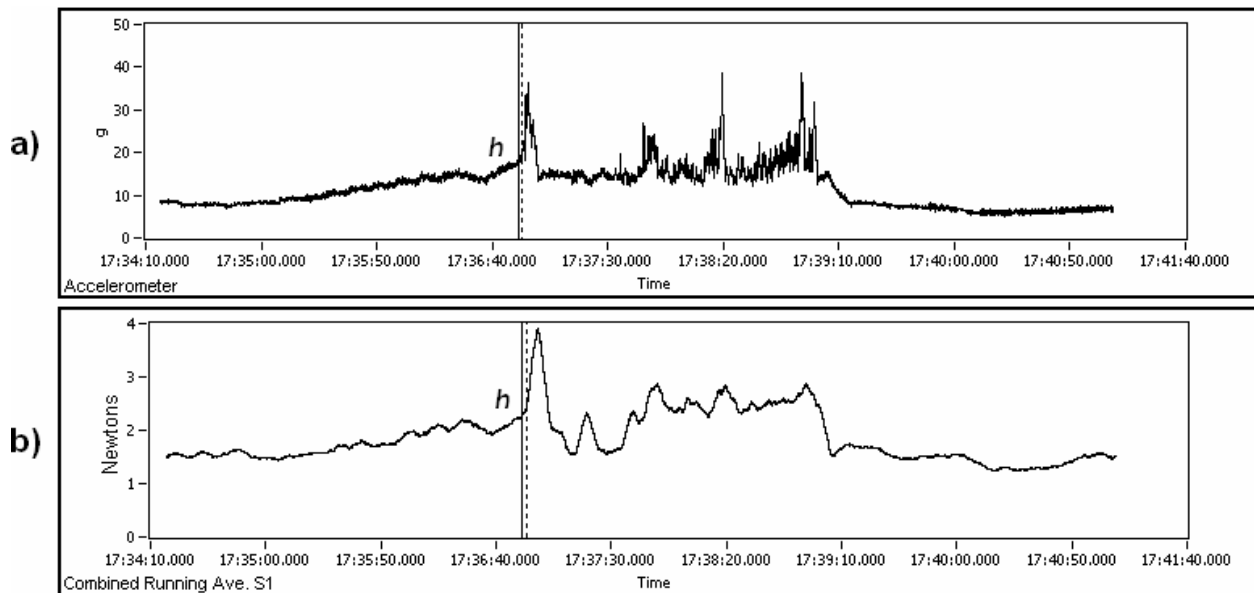


**Figure 12. Detail of event *h* in a) the accelerometer data and b) the RFS data. The sudden increase in forces leads to a relatively small lead time for this event.**

The sensitivity results in Figure 9 show that the accelerometer based system cannot outperform the RFS for more than one event without also causing false triggers. The event for which the RFS system lags is suspected to be an interrupted clash and occurs at relatively low force amplitude. The study also shows a decrease in average lead time from the RFS as the accelerometer offset is reduced from its initial value. Despite this reduction in advantage, the RFS still outperforms the accelerometer by a significant margin.

The sensitivity results shown in Figure 10 show that any increase in the RFS alarm offset results in a reduction in the average lead time. However, the RFS system is still able to pre-detect all events for offsets up to 0.22 N. When the offset is further increased to 0.23 N, two events show negative lead times. The average lead time of these two events is -1.65 s. This negative lead time is small when compared to the remaining seven events, whose average lead time is 9.45 s. As the offset is further increased in increments to 0.26 N, the average lead time of these two events decreases to -2.13 s. However, this is still small compared to the average lead time of 8.93 s for the remaining seven events. A decrease in the RFS offset below 0.20 N results in an increase in the average lead time, but is accompanied by false triggers.

## CONCLUSIONS

Four Refiner Force Sensors (RFS) were installed in a mill-scale pulp refiner at the Catalyst Paper mill in Port Alberni, B.C., Canada. These sensors replace a short segment of a refiner bar and measure normal forces and tangential shear forces that are applied to the bar by the pulp. The refiner used for these experiments is an Andritz 45-1B refiner which is a single-disc type. The sensors were installed at different locations along the same radius in a Durametal™ 47209 plate segment. The experiments were performed over a three-month period starting in September of 2005. Data was collected at regular intervals over the installation and consisted of four day-long trials of continuous collection and four long periods of intermittent, short term data collection intervals. In total, the data collected contains 9 clash events all of which occurred in the first day of testing.

The data recorded from the sensors was processed to detect the onset of refiner plate clash. Several methods of processing the data to produce a predictive tool were explored. These methods included a running count of the density of high force peaks, a weighted version of the peak density method which also accounted for peak height, the running average of RFS data, and the combined running average of RFS data based on the average of the forces measured by one or more sensors. Of the methods explored, the combined running average yielded the best performance.

The combined running average algorithm computes the running averages of the RFS shear and normal force signals. These running averages are then averaged, producing a single signal. The combined running average of the shear and normal force signals from S1 can predict all events before the accelerometer-based system with an average lead of 10.9 s. Sensor 2 through 4 could also predict all the events but not with the same performance as S1. It is speculated that this is due to S1's unique location on the refiner plate, inside of the stagnation point.

A sensitivity study revealed that the accelerometer could not match the performance of the RFS for any event, other than one, without also causing false triggers. The study also showed that the RFS system could offer improved detection performance for a broad range of offset values.

## References

1. Allison, B.J., Ciarniello, J.E., Tessier, P.J.C. and Dumont, G.A., "Dual adaptive control of chip refiner motor load", *Pulp Paper Can.*, 96(3), pp. 39(1995).
2. Dumont, G.A. and Astrom, K.J., "Wood chip refiner control", *IEEE Control Systems Magazine*, 8(2), pp. 38(1988).
3. Jack, J.S., Mills, C. and Baas, P.H., "A device for detection and prevention of plate clash in disc refiners", *Pulp Paper Can.*, 82(9), pp. 89(1981).
4. Rogers, J.H. and Butler, D.J., "Method and system for detecting plate clashing in disk refiners", United States Patent 4,233,600, issued November 11(1977).
5. Whyte, D.M., "Methods of and/or apparatus for detecting and controlling refiner plate clashing", United States patent 4,627,578, issued December 9(1986).

6. Brenholdt, I. R., "Apparatus and method for particle size classification and measurement of the number and severity of particle impacts during comminution of wood chips, wood pulp and other materials", United States Patent 5,605,290, issued February 25(1997).
7. Siadat, A., Bankes, A., Wild P.M., Senger, J. and Ouellet, D., "Development of a piezoelectric force sensor for a chip refiner", Proc IMechE Part E: Journal of Process Mechanical Engineering, 217(2), 133(2003).
8. Senger, J., Ouellet, D., Wild, P., Byrnes, P., Sabourin, M. and Olender, D., "A technique to measure mean residence time in TMP refiners based on inherent process fluctuations", J. Pulp Paper Sci., 32(2), pp. 83 (2006).

# Refiner Force Sensor Project:

**Paper 1:** Forces on Bars in High-consistency Mill-scale refiners: Effect of Consistency

**Paper 2:** Refiner Plate Clash Detection Using an Embedded Force Sensor

Presented by: Dustin Olender

Co-authors: Peter Wild, Paul Francescutti, Peter Byrnes, Daniel Ouellet, and Marc Sabourin

Partners:



University  
of Victoria



Paprican

ANDRITZ



NSERC  
CRSNG

IMPC 2007





# Outline

## ◀ Paper 1: Effect of Consistency

- Introduction
- Experiments
- Signal Processing
- Results and Discussion

## ◀ Paper 2: Plate Clash Detection

- Introduction
- Signal Processing
- Results and Discussion



# Introduction: Background

## ◀ Laboratory single-bar refiner:

- Found a relationship between impact shear forces and floc consistency
- Defined the *equivalent tangential coefficient of friction*  $\mu_{teq}$  as average shear divided by average normal force
- Flocs with consistencies above 35% were shown to have positive correlation with  $\mu_{teq}$



# Introduction: RFS4 Trials

## ◀ Springfield, OH

The logo for ANDRITZ, featuring the word "ANDRITZ" in white capital letters on a blue background with diagonal lines.

- Qualify RFS4 in pressurized 36-1CP refiner
- Test consistency

## ◀ Port Alberni, BC

The logo for Catalyst, featuring the word "Catalyst" in red lowercase letters next to a red and white striped graphic.

- Qualify long-term operation of RFS4 in 45-1B
- Test consistency



Close-up of RFS4 installed in 45-1B in Port Alberni



# Outline

## ◀ Paper 1: Effect of Consistency

- Introduction
- Experiments
- Signal Processing
- Results and Discussion

## ◀ Paper 2: Plate Clash Detection

- Introduction
- Signal Processing
- Results and Discussion



# Experiments: Installation

Springfield, OH



Installation of instrumented 36604 plate



◀ RFS installed through rear of plate



# Experiments: Installation

Springfield, OH



► 7 o'clock position



Location of instrumented plate in 36-1CP stator



# Experiments: Installation

Springfield, OH



- ▶ 3 sensors positioned evenly throughout refining zone



Identification of RFS in 36604 plate



# Experiments: Trial Plan

Springfield, OH



- ◀ Spruce chips were refined
- ◀ Four (4) dilution flow rates, at two (2) different motor loads
- ◀ Dilution flow rate: 5 – 11 USGPM
- ◀ Motor loads: 650 kW – 800 kW
- ◀ Refiner speed: 1900 RPM



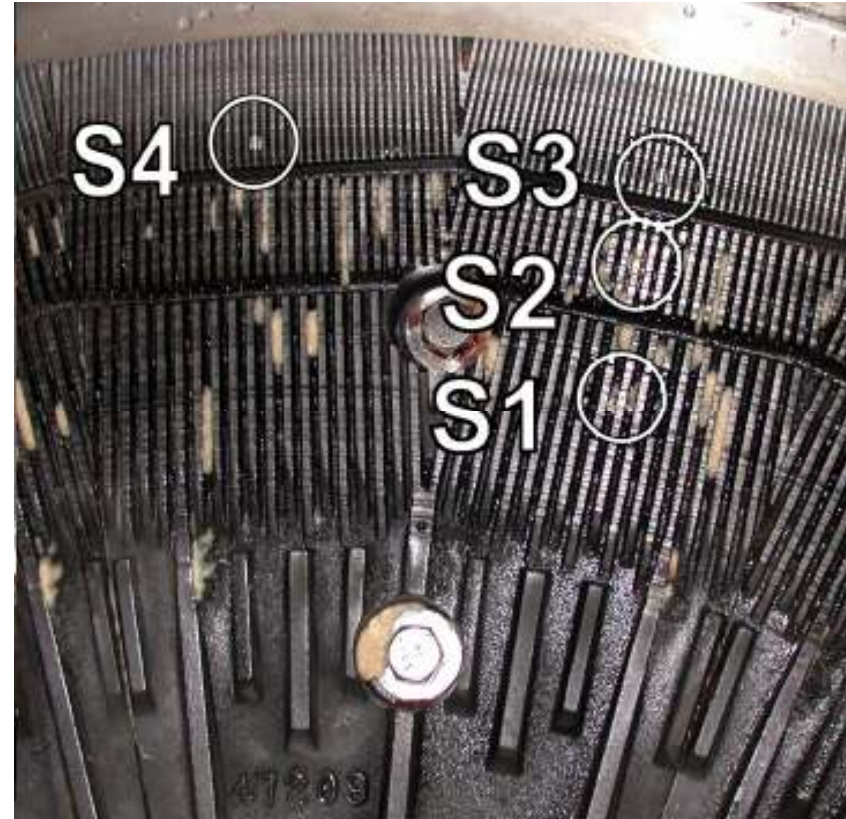


# Experiments: Installation

Port Alberni, BC



- ▶ 3 sensors +1 redundant at outer radius



Identification of RFS in 47209 plate



# Experiments: Trial Plan

Port Alberni, BC



- ◀ CTMP Rejects Pulp
- ◀ Dilution flow rate(3 – 7 USGPM) and speed of dewatering press at constant motor load (3 MW)
- ◀ Refiner speed: 1800 RPM



# Outline

## ◀ Paper 1: Effect of Consistency

- Introduction
- Experiments
- **Signal Processing**
- Results and Discussion

## ◀ Paper 2: Plate Clash Detection

- Introduction
- Signal Processing
- Results and Discussion



## Signal Processing:

- ◀ Software used to isolate and catalogue individual bar-crossing
- ◀  $\mu_{teq}$  calculated for each bar-crossing
- ◀ Mean  $\mu_{teq}$  calculated from three 5-second samples (100 000s of bar-crossings)



# Outline

## ◀ Paper 1: Effect of Consistency

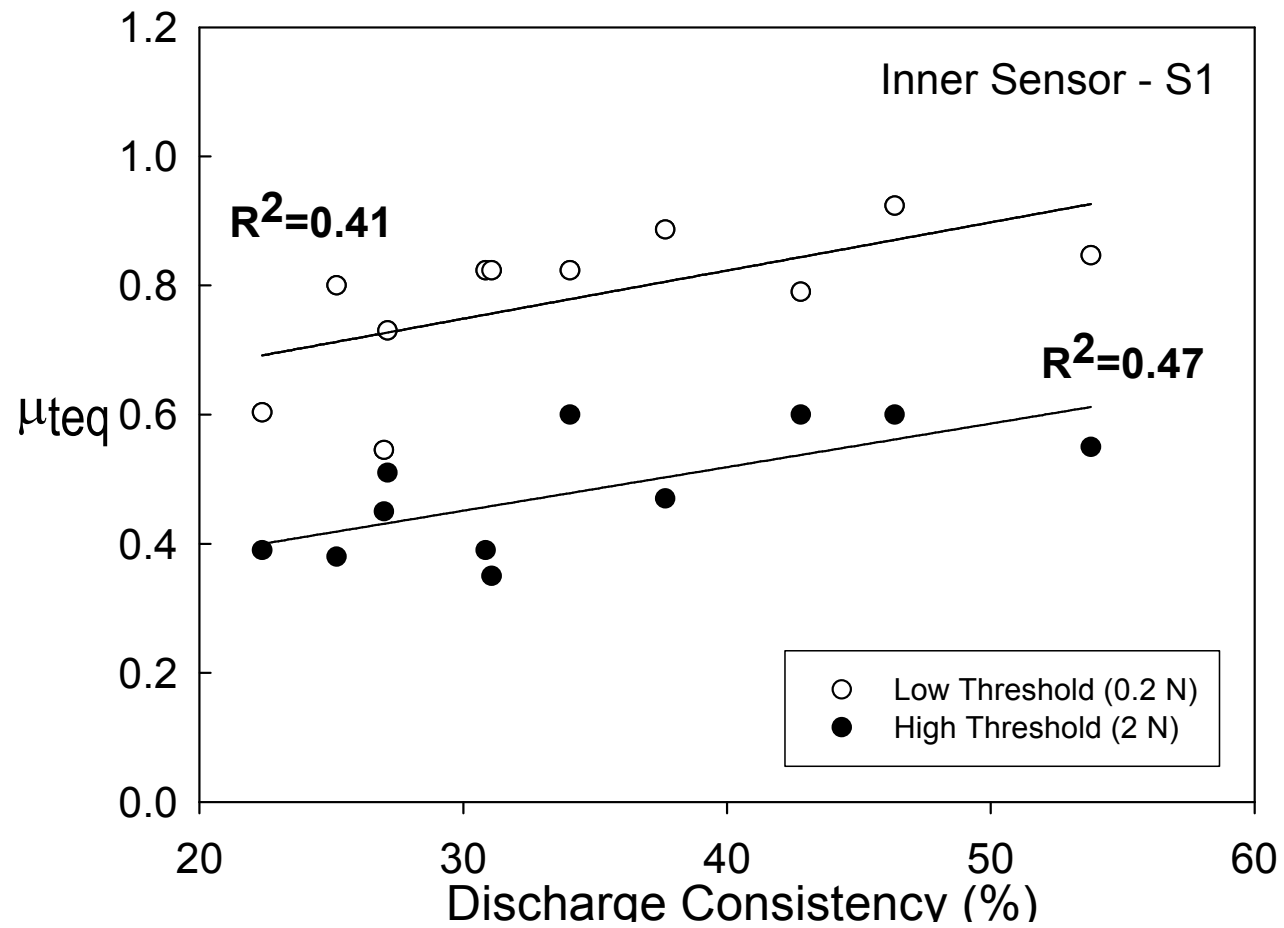
- Introduction
- Experiments
- Signal Processing
- Results and Discussion

## ◀ Paper 2: Plate Clash Detection

- Introduction
- Signal Processing
- Results and Discussion

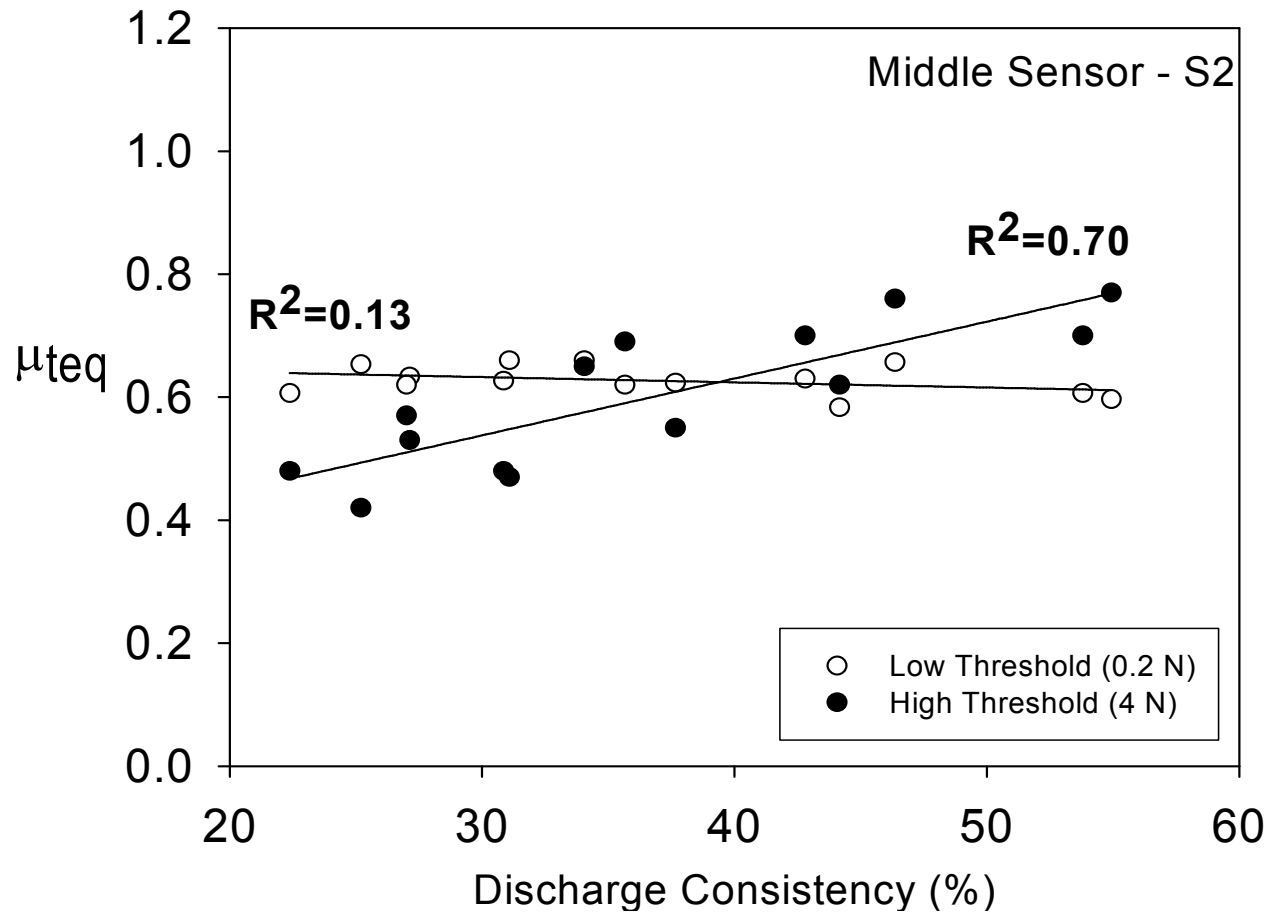


# Results: Springfield



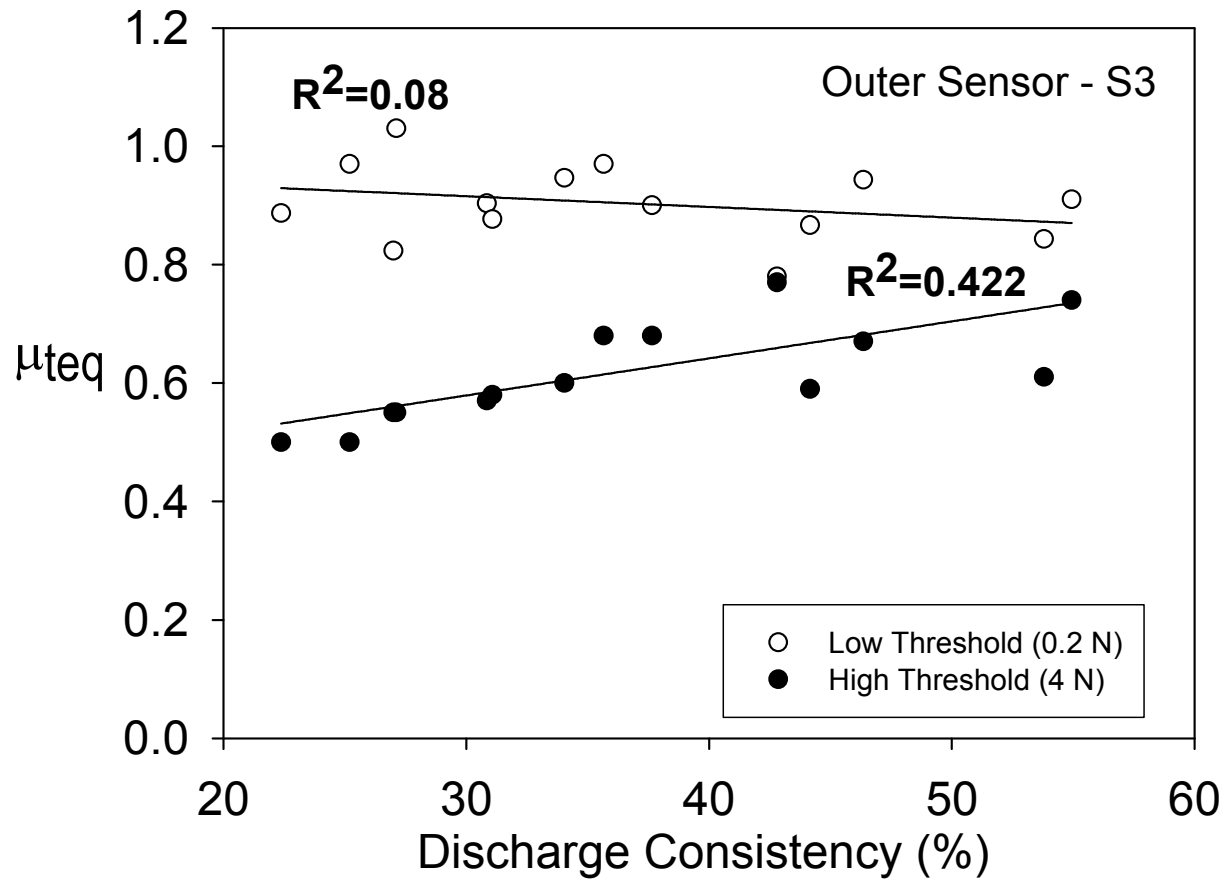


# Results: Springfield





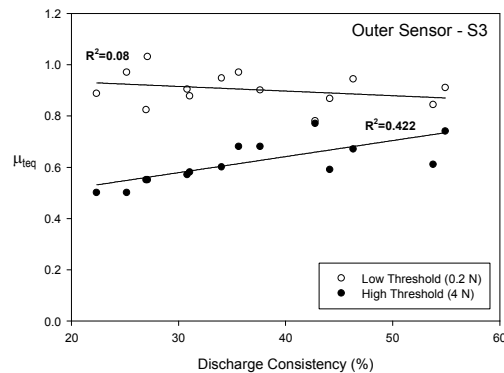
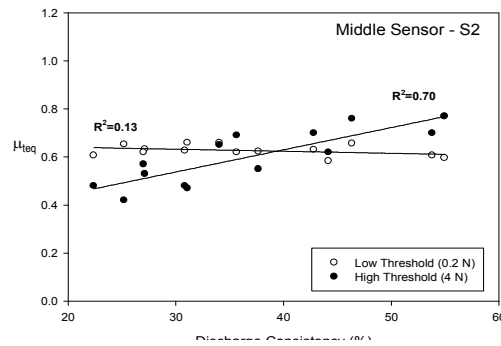
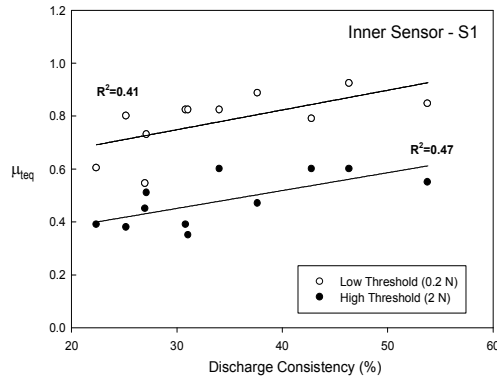
# Results: Springfield







# Discussion: Springfield

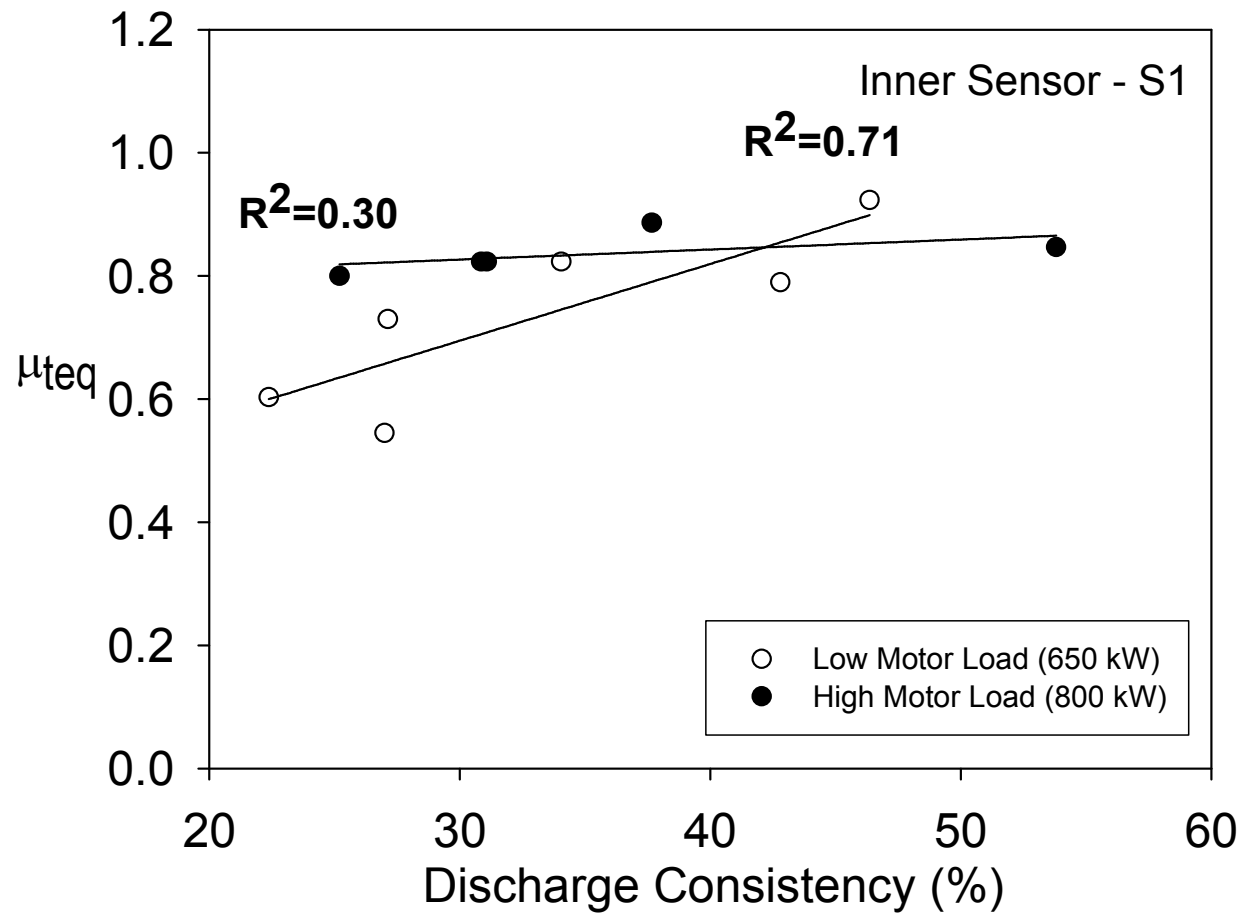


## Inner Sensor Sensitivity:

- ◀ Thicker grammage flocs were shown to increase sensitivity to  $\mu_{teq}$  in laboratory experiments
- ◀ Inner sensor encounters thicker, more intact fibre bundles, such as shives

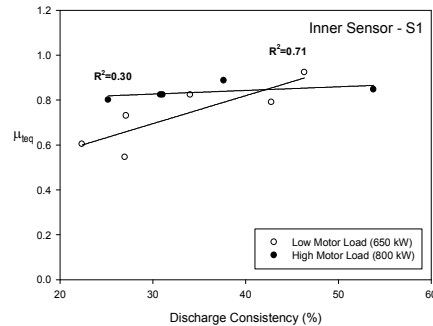


# Results: Springfield





# Discussion: Springfield



## Low Motor Loads:

◀ Low motor loads saw increased sensitivity to  $\mu_{teq}$

◀ More research is necessary



## Results: Port Alberni

- ◀ No significant changes in  $\mu_{teq}$  recorded over experiments
- ◀  $\mu_{teq}$  recorded at inner, middle and outer sensors: 0.34, 0.64, and 0.53.



## Discussion: Port Alberni



### **No Change in $\mu_{teq}$ :**

- ◀ Recorded discharge consistencies (20-27%) below 35% threshold
- ◀ Shear forces unchanged in flocs with consistency below 35% in laboratory
- ◀ Small range of consistencies could also be a factor



# Outline

## ◀ Paper 1: Effect of Consistency

- Introduction
- Experiments
- Signal Processing
- Results and Discussion

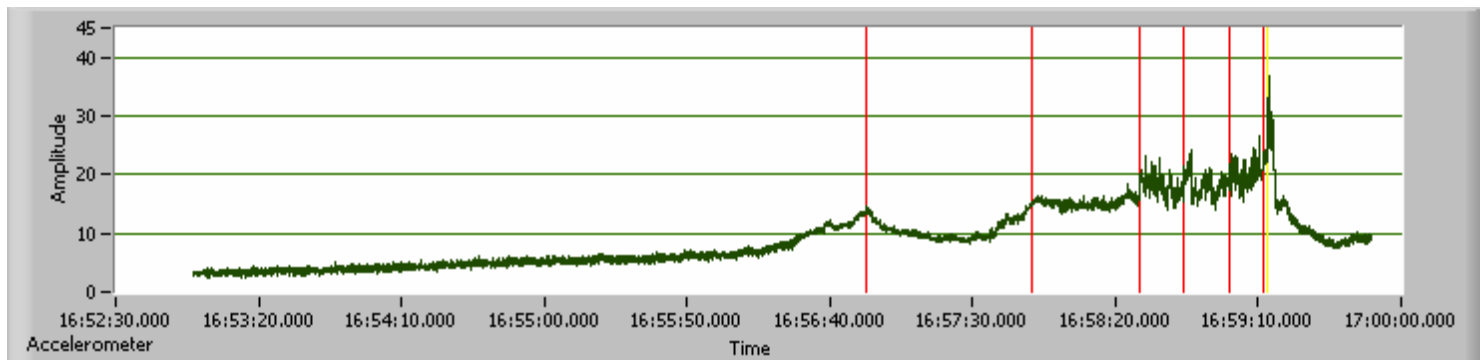
## ◀ Paper 2: Plate Clash Detection

- Introduction
- Signal Processing
- Results and Discussion



# Introduction: Current Plate Protection System

- ◀ Current system consists of two alarms based on data collected from an accelerometer mounted on the refiner.
  - **Alert:** The plates are opened when the accelerometer signal exceeds a set threshold.
  - **Danger:** The plates are opened when the accelerometer signal exceeds a running average by a set threshold.





# Outline

## ◀ Paper 1: Effect of Consistency

- Introduction
- Experiments
- Signal Processing
- Results and Discussion

## ◀ Paper 2: Plate Clash Detection

- Introduction
- Signal Processing
- Results and Discussion





# Signal Processing: Detection Methods

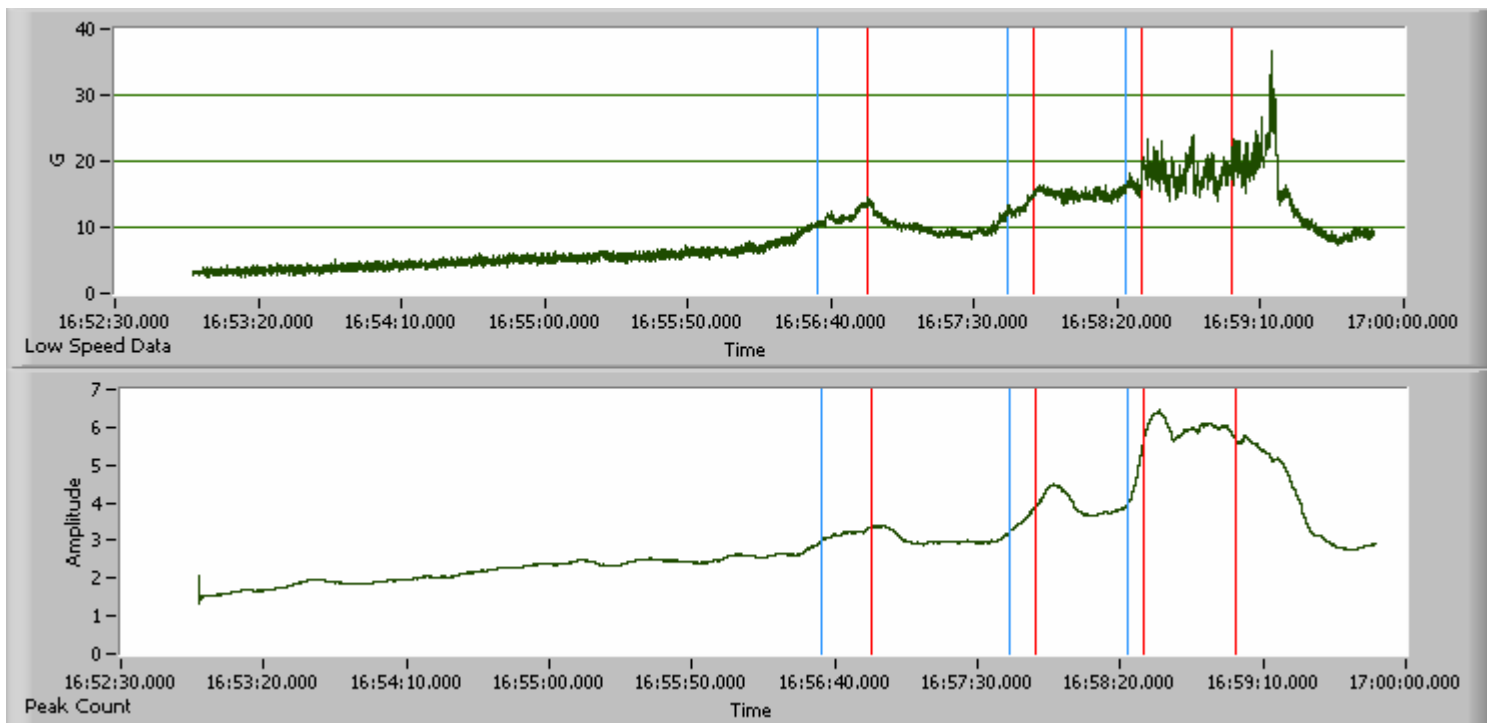
- ◀ Using the RFS data to generate a trend which can be monitored for clash detection.
  - Reduce sample rate and rectify data.
  - Calculate the running average of the RFS data for each data curve (2 per sensor).
  - Compare the curve to a dynamic threshold.



# Signal Processing: Detection Method Cont'd

## ◀ One sensor used to predict clash

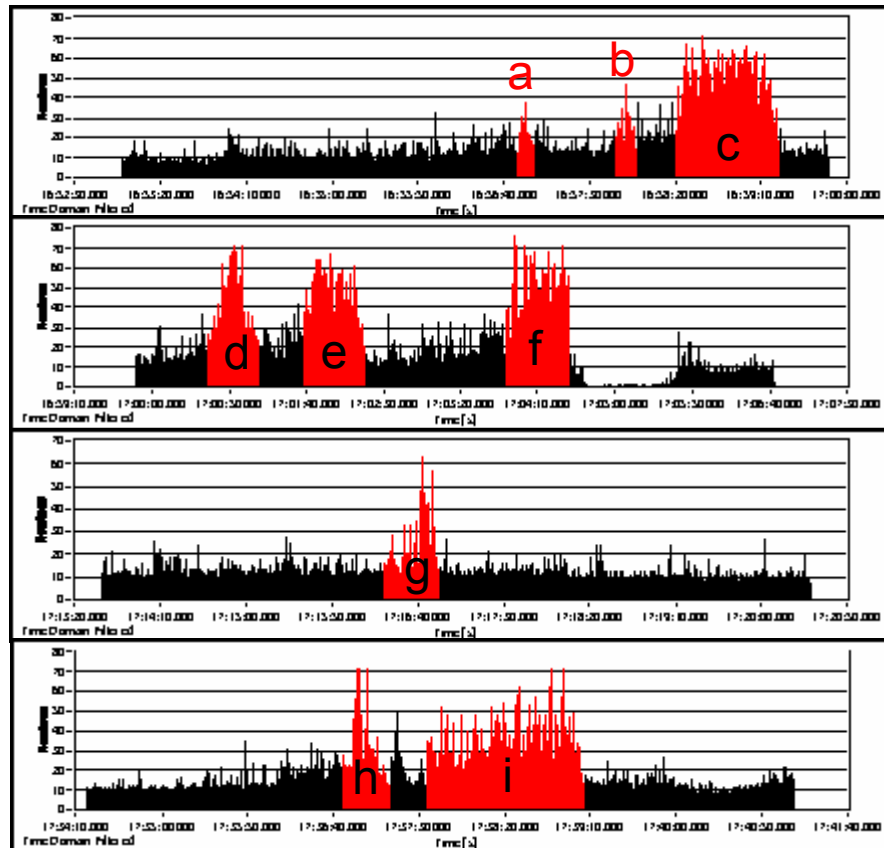
- Curve generated from average of Normal and shear force.
- Threshold is based a 15 s running average.





# Results: Clash Detection

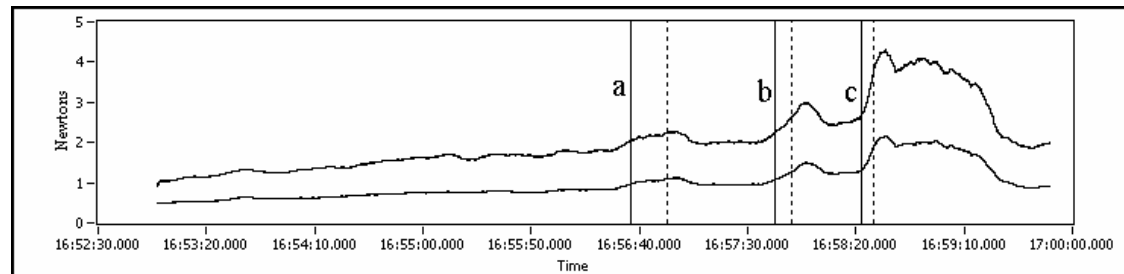
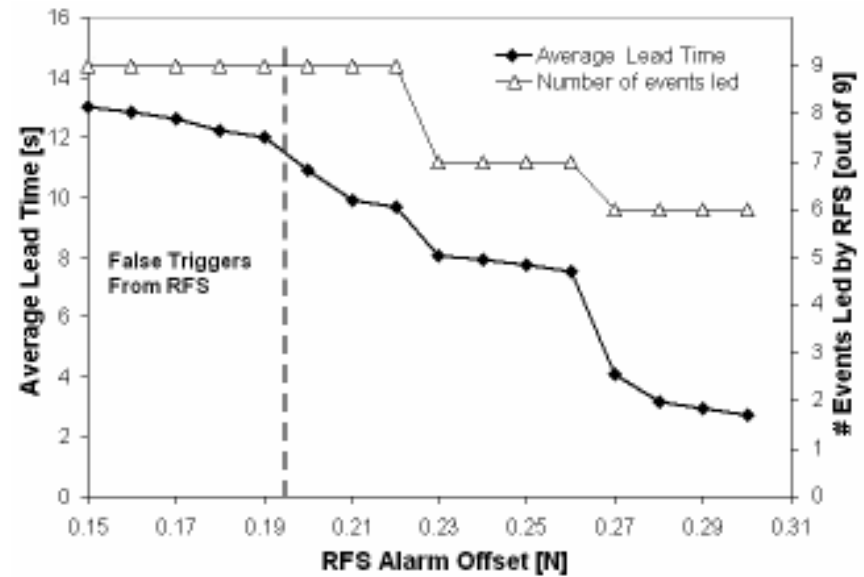
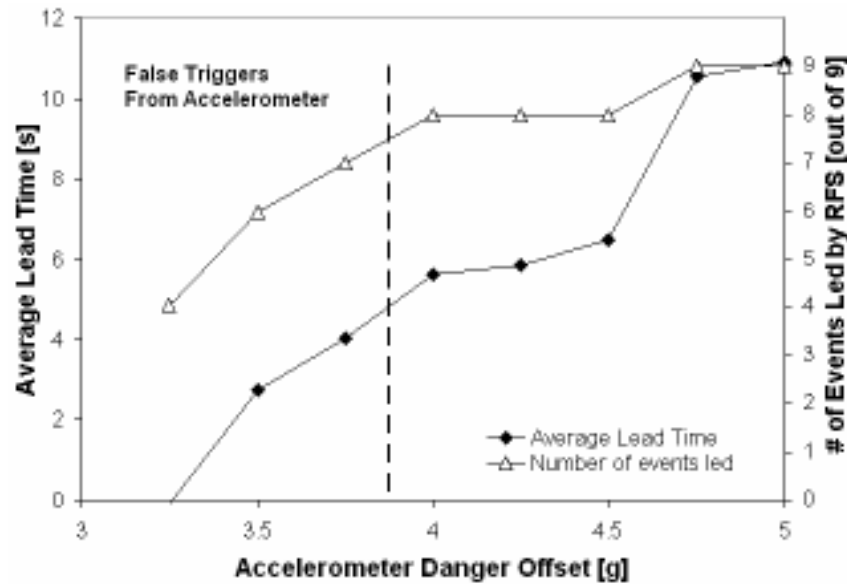
◀ RFS clash detection was able to predict all clash events before the accelerometer system.



Event	RFS lead [s]
a	12.9
b	9.3
c	6.1
d	7.5
e	24.7
f	11.2
g	15.9
h	21.86
i	8.71
<b>average</b>	<b>10.9</b>



# Results: Sensitivity Study





## Conclusions: Clash Detection

- ◀ The RFS sensor was able to predict a clash several seconds before the current accelerometer-based system.
- ◀ Sensitivity study showed that the accelerometer could not match the RFS clash detection without producing false triggers.



Thank-you  
&  
Questions?



# Springfield Trial Plan

Σαμπλε ΙΔ	Ταργετ Μοτορ Λοαδ (κΩ)	Προδ. Ρατε (τ/δ)	Σπεχιφιχ Ενεργγψ (κΩη/τ)	Πλατε Γαπ (μμ)	Δισχηαργε Χονσιστ. (%)
A15	550	21.1	562	0.76	
A16	650		673	0.56	
A17	750		721	0.43	
A18	850		899	0.25	
A19	450	18.4	505	1.07	
A20	550		626	0.94	
A21	650		702	0.74	
A22	750		891	0.46	
A23	600	26.4	521	0.94	
A24	700		620	0.64	
A25	800		701	0.53	
A26	900		796	0.36	



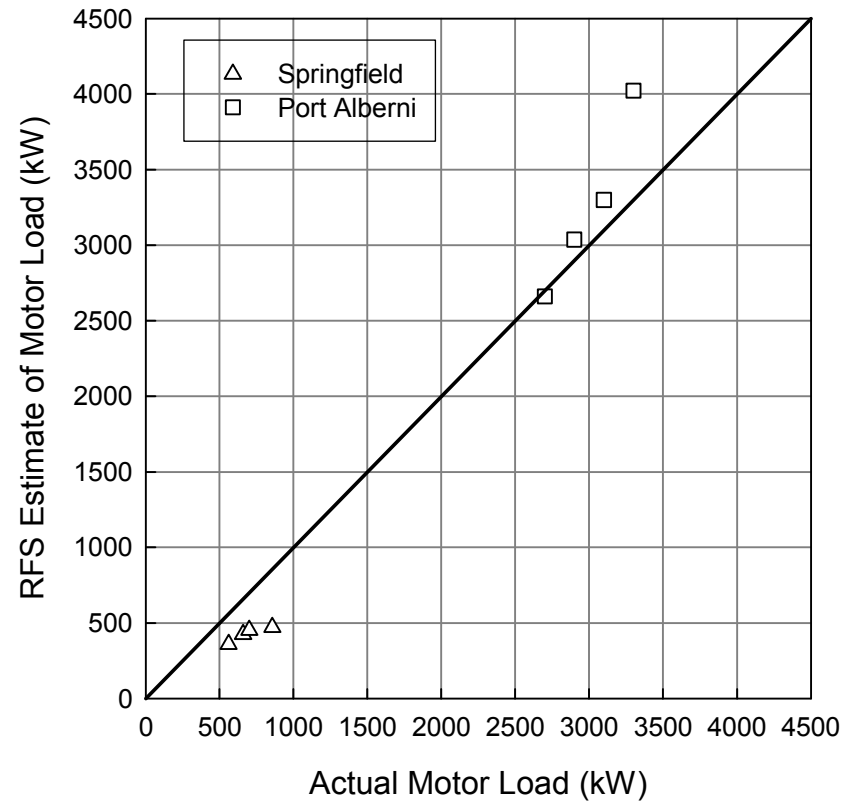
# Port Alberni Trial Plan

Σαμπλε ΙΔ	Μοτορ Λοαδ (κΩ)	Προδ. Ρατε (οδμτ/δ)	Σπεχιφιχ Ενεργψ (κΩη/τ)
A1	2700	61.2	1055
A2	2900		1137
A3	3100		1216
A4	3300		1294
A5	3000	55.0	1309
A6		59.3	1214
A7		61.4	1173
A8		65.5	1099





# Shear Work: Power Estimate





# Experiments: Installation

Port Alberni, BC



Wire routing to 45-1B refiner at Port Alberni



- ◀ Pre-installation of ancillary equipment one week prior
- ◀ Main installation during routine plate change



# Experiments: Installation

Port Alberni, BC



◀ Instrumented plate installed at 2 o'clock

Stator awaiting plate on 45-1B refiner